



# Effect of fluorine on the phase formation and superconducting properties of Tl-1223 superconductors

N.M. Hamdan \*, Kh.A. Ziq, A.S. Al-Harhi

*Physics Department, King Fahd University of Petroleum and Minerals, Dhahran, 31261, Saudi Arabia*

Received 23 February 1998; revised 2 December 1998; accepted 4 January 1999

## Abstract

Fluorination of  $(\text{Tl}_{0.5}, \text{Pb}_{0.5})\text{Sr}_{1.6}\text{Ba}_{0.4}\text{Ca}_2\text{Cu}_3\text{O}_y$  high-temperature superconductors has been performed through partial replacement of CuO by  $\text{CuF}_2$  in the starting materials. Seven samples with nominal fluorine content  $x$  atom per formula unit ( $0 \leq x \leq 3.6$ ) were examined by X-ray diffraction (XRD), scanning electron microscopy (SEM), resistivity and magnetization  $M(H)$  measurements. Fluorine addition has raised the onset transition temperature to 128 K, and increased the critical current density to 300%, the value of the fluorine free sample. XRD, SEM and energy dispersive X-ray (EDX) results showed that the formation of the Tl-1223 phase was enhanced as fluorine was introduced, and the formation of large grains was observed. EDX spot analysis revealed the presence of fluorine as a species of the structure of the Tl-1223 grains. The  $c$ -axis of Tl-1223 decreased with increasing  $x$ , indicating that fluorine had replaced oxygen in the structure. The behavior of the normal state resistivity with temperature indicated that fluorine addition changed this material from overdoped to optimally doped, and upon further fluorine addition, changes it to slightly underdoped state. That provided an additional evidence that fluorine addition changes the density of charge carrier concentration in the Cu–O planes and improves the superconducting properties of this material. © 1999 Published by Elsevier Science B.V. All rights reserved.

PACS: 74.1; 74.3C; 74.6G; 74.6M

Keywords: Fluorination; Overdoped; Tl-1223; Hole concentration

## 1. Introduction

Charge carrier concentration in the Cu–O planes plays an important role in high  $T_c$  superconductors [1–4]. The  $\text{TlBa}_2\text{Ca}_2\text{Cu}_3\text{O}_9$  (Tl-1223) phase is among other thallium-based superconductors that fall in the overdoped region where Cu valency is more than two [1]. Optimizing the hole concentration in the Cu–O planes has been seen to improve the

superconducting properties of these compounds [3–5].

There have been successful attempts to decrease the hole concentration in the Cu–O planes of Tl-based superconductors, through either cation substitution of cations that have higher valencies or through oxygen non-stoichiometry [1,2,6,7]. Anion substitution for oxygen, of anions that are more electronegative, such as fluorine, may also reduce the hole concentration, and affect the superconducting properties of this compound. Fluorine may only substitute oxygen in the structure because of its comparable

\* Corresponding author. Fax: +966-3-860-2293; E-mail: nmhamdan@kfupm.edu.sa

ionic radii ( $r(\text{F}^-) = 0.136$  nm and  $r(\text{O}^{2-}) = 0.14$  nm), while cations can go into more than one site and may cause effects other than decreasing the hole concentration. To our knowledge, very few attempts have been made to introduce fluorine into the Tl-1223 superconducting phase. Moreover, no conclusive evidence has been published that confirms that fluorine replaces oxygen in high- $T_c$  superconductors, other than the electronic  $\text{Nd}_2\text{CuO}_4$  superconductor [8–18].

Tachikawa et al. [19] have reported that fluorine addition promotes the phase transformation from Tl-2223 to Tl-1223 phase, and improves the critical current density in the diffusion layer of fluorine. The Kansas group [20] has found that fluorine doping to the non-superconductor, Tl-1212, converts it to a superconductor, although the group has not confirmed that fluorine is incorporated into the structure, but affects the hole carrier concentration [20]. In a later work, the same group observed an increase in  $T_c$  of Tl-2201 phase, and has concluded from Mössbauer results that fluorine could have replaced oxygen in the crystal lattice [21]. Recently, Bellingeri et al. [22] have found that the phase formation of Tl-1223 has been improved with fluorine addition. Furthermore, they have observed an increase of the irreversibility line, and a slight improvement in the field dependence of the critical current density with fluorine inclusions. We have previously reported that the addition of fluorine has increased the critical currents and improved the formation of Tl-1223 phase [23–25].

In this paper, we report further results which support that fluorine is being incorporated in the structure of the Tl-1223 phase and its effect on the phase formation, structure, microstructure, magnetic and transport properties of the  $(\text{Tl}_{0.5}\text{Pb}_{0.5})(\text{Sr}, \text{Ba})_2\text{Ca}_2\text{Cu}_3\text{O}_y$  (Tl-1223) system.

## 2. Experimental

Tl-1223 high-temperature superconductors were prepared at ambient atmosphere using the solid state reaction technique. Precursors were prepared from high purity  $\text{CuO}$ ,  $\text{Sr}(\text{NO}_3)_2$ ,  $\text{CaO}$  and  $\text{BaO}_2$  mixed according to the formula  $(\text{Tl}_{0.5}\text{Pb}_{0.5})\text{Sr}_{1.73}\text{Ba}_{0.43}\text{Ca}_{2.16}\text{Cu}_3\text{O}_y/\text{F}_x$ , where  $(0 \leq x \leq 3.6)$ . The mixtures were heated to  $800^\circ\text{C}$  at  $5^\circ\text{C}/\text{min}$ , followed by

intermediate grinding and heating slowly to  $970^\circ\text{C}$ , and annealed for 15 h. The precursor was mixed with following molar ratios:  $x\text{CuF}_2$ ,  $0.5\text{PbO}$  and  $0.35\text{Tl}_2\text{O}_3$  and heated at  $5^\circ\text{C}/\text{min}$  to  $800^\circ\text{C}$  for 10 h. The temperature was then increased slowly ( $2^\circ\text{C}/\text{min}$ ) to  $980^\circ\text{C}$  and maintained for 10 min. The temperature was then decreased at  $2^\circ\text{C}/\text{min}$  to  $880^\circ\text{C}$  and maintained for 33 h. The heating at  $980^\circ\text{C}$  for 10 min caused partial melting of the samples. We started with 0.35 mol of  $\text{Tl}_2\text{O}_3$  instead of 0.25 mol, as part of it will evaporate at elevated temperatures.

Five samples with different fluorine content  $x$  atoms per formula unit were prepared according to the above-mentioned procedure and annealed in air. Two more samples with  $x = 3.0$  and  $3.6$  were annealed in oxygen flowing atmosphere. The resulting samples have been characterized using standard four probes resistance and DC magnetic measurements. Hysteresis loops were obtained using 9 T vibrating sample magnetometer.

Structure analysis has been done using the X-ray diffraction (XRD) technique on a Phillips 1700 diffractometer with  $\text{Co K}\alpha$  radiation with wavelength of 0.17890 nm. Scanning electron microscopy (SEM) and energy dispersive X-ray (EDX) spectroscopy were performed on a JEOL 5800 microscope, with a beryllium window which can distinguish light elements down to carbon. The accelerating voltage of the electrons was 20 kV. Imaging was done in a backscattered electron mode since it provided a good contrast of the phases due to the difference in average molecular weight of each phase.

## 3. Results and discussion

### 3.1. Structure and microstructure

X-ray diffraction patterns for samples with different fluorine contents  $x$  are shown in Fig. 1. The figure shows clearly that the peaks of the Tl-1223 phase dominated the Tl-1212 phase as fluorine was increased. The phase purity of the Tl-1223 increased from about 30% to about 70% as fluorine was increased, consistent with recent results of Bellingeri et al. [22] ( $\approx 65\%$ ) obtained for fluorine doping of the same system using a different preparation route. Traces of  $(\text{CaSr})_2\text{PbO}_4$  and  $(\text{CaSr})_2\text{CuO}_3$  that are

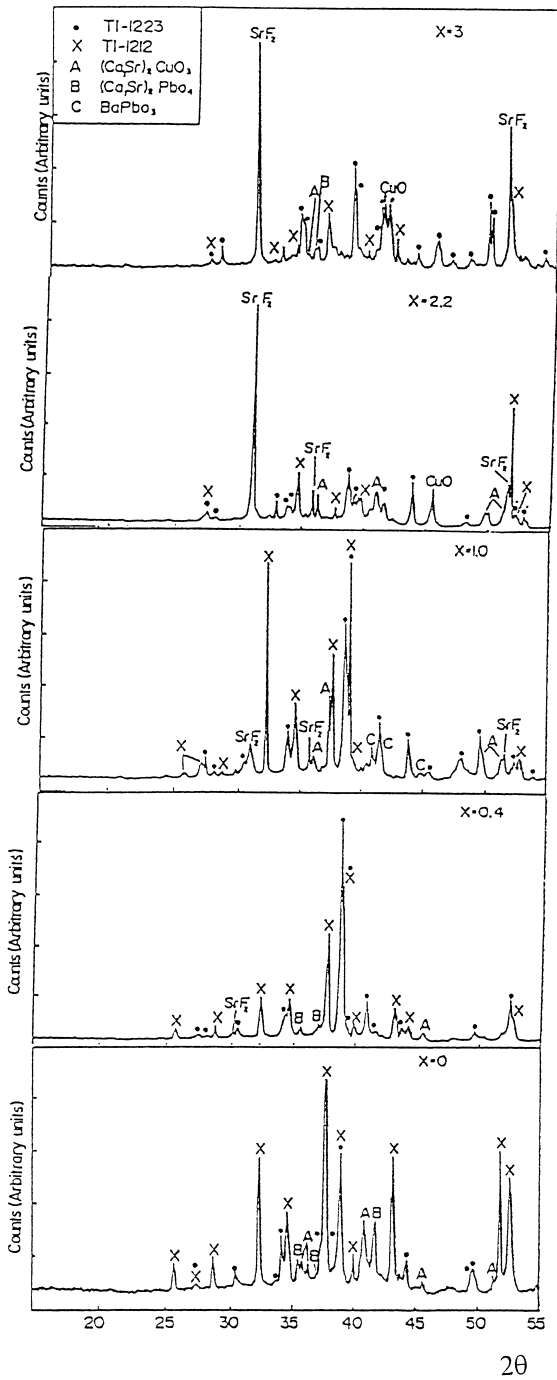


Fig. 1. The XRD pattern for the samples with different fluorine contents,  $x$ .

commonly seen in Tl-based materials [22,26,27] were also observed. Traces of  $BaPbO_3$  were observed only

in the XRD spectrum of the sample with  $x = 1.0$ .  $SrF_2$  started to appear for  $x \geq 0.4$ . Adding more  $CuF_2$  promotes the formation of  $SrF_2$  in larger amounts (as seen from XRD), and increases the chance of formation of other impurity phases. Traces of the  $CuO$  phase started appearing for  $x = 2.2$  and 3, which were absent in the XRD patterns of the precursor of all the samples. This would indicate that the observed  $CuO$  traces in the fluorinated Tl-1223, had been formed during the final stages of annealing only when the fluorine content was above 2.2. It should be noted that, for a complex material like Tl-1223, XRD is usually sensitive for traces of the order of 5% of the bulk.

Refinement of the lattice parameters of all phases has been done using the PDP XRD analysis package [28]. Fig. 2 shows the variation of the  $c$ -axis of Tl-1223 lattice with starting fluorine content  $x$ . The reduction of the  $c$ -axis with fluorine addition is one piece of evidence that supports the idea that fluorine enters the structure of the superconducting Tl-1223 phase. The strong electronegativity and smaller ionic radius of fluorine may cause fluorine to partially substitute oxygen. This is in line with previous results obtained for the Bi-based and Hg-based superconductors [29,30,17,31,32].

Fig. 3 presents SEM micrographs for different samples. The formation of large grains (up to more than  $100 \mu m$ ) in these samples was observed. EDX spot analysis was performed for 10 different grains

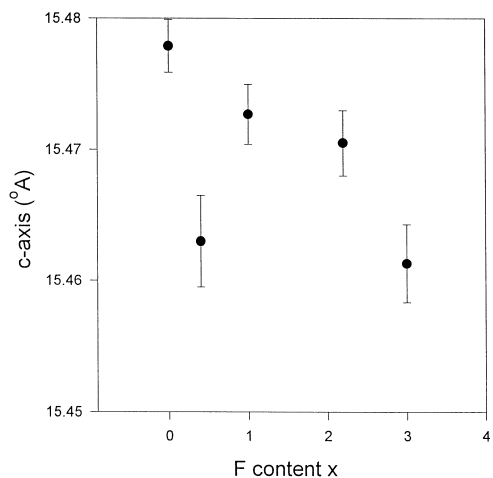


Fig. 2. Variation of the refined  $c$ -axis with fluorine content,  $x$ .



Fig. 3. The SEM micrographs for samples with  $x = 1.0, 2.2$  and  $3.0$  from top to bottom, respectively. The scale marker is  $20 \mu\text{m}$ .

in each micrograph. The grain size of most of the investigated grains was at least  $20 \mu\text{m}$ , while the beam diameter was about  $3 \mu\text{m}$ . This ensures that the spectrum that we have observed is coming from the grain itself and not from the intra-grain boundary. The contrast in the backscattered electron beam

image is proportional to the molecular weight of each grain, therefore, different phases will produce images with different contrasts.

Elemental analysis of EDX spectrum of the grains qualitatively agrees with phases that had been detected by XRD patterns presented in Fig. 1. In addition, grains of the Tl-1223 phase contained a very clear fluorine peak, as can be seen in Fig. 4. The observed fluorine peaks from the spectrum of the superconducting Tl-1223 phase provide an additional evidence that fluorine enters the structure of Tl-1223 phase. Since samples were not polished, the intensity of the EDX peak of each element depends on the angle that the backscattered electron beam makes with the grain. However, the relative intensities of the peaks of each element qualitatively agree with preliminary results obtained for polished samples.<sup>1</sup> Polishing was not performed intentionally in order to clearly observe the grain size and boundaries.

### 3.2. Transport properties

Fig. 5 shows the resistivity curves as a function of temperature for samples with different nominal fluorine contents, annealed in air. The figure shows that the transition temperature of the fluorine-doped samples is consistently higher than that for the fluorine-free sample. The figure also reveals that the transition becomes sharper for fluorine-doped samples. The variation in the transition temperature  $T_c$  with fluorine content  $x$  is shown in Fig. 6.  $T_c$  in this figure was obtained from the position of the peak in the graph of the derivative of the resistivity  $\rho$  vs. temperature  $T$  [ $(d\rho/dT)$  vs.  $T$ ]. The figure shows that  $T_c$  increases with increasing fluorine content, reaching a maximum value of  $128 \text{ K}$  at  $x = 1$  above which  $T_c$  starts decreasing. A further increase occurred in  $T_c$  for the sample with  $x = 3$  accompanied by an increase in the transition width of this sample. The transition width  $\Delta T_c$  decreased rapidly as fluorine was increased from zero to  $x = 0.4$ , where it

<sup>1</sup> We have performed SEM and EDX measurements on polished samples that revealed similar results. These data are under analysis.

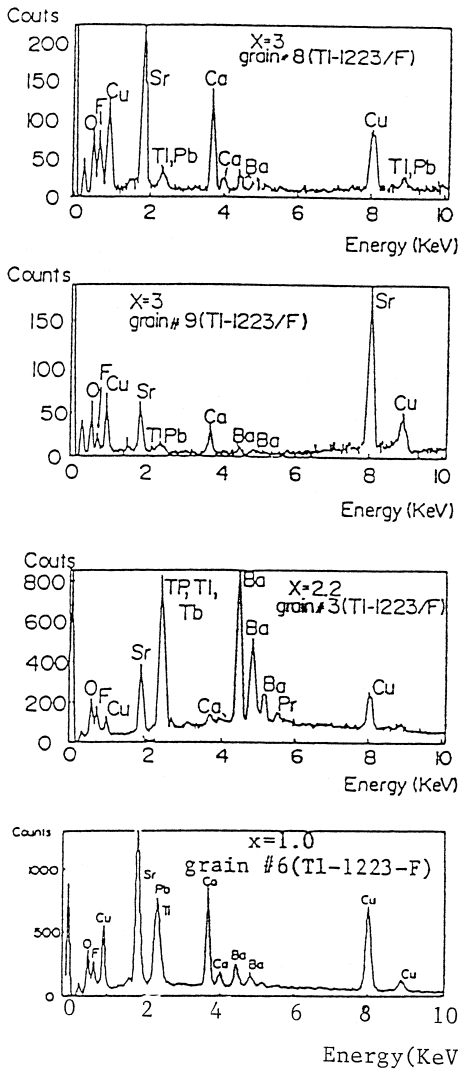


Fig. 4. The EDX spectra of the Tl-1223 phase which contains fluorine for the three samples in Fig. 3, corresponding to the grains marked in the micrographs.

reached a value less than 1.5 K, then it increased gradually as fluorine content was increased, reaching a value larger than that for the fluorine-free sample. These results are consistent with the variation of the *c*-axis with fluorine content (Fig. 2), where the *c*-axis of the sample with  $x = 0.4$  had considerably decreased as compared with all other samples. The increase in transition temperature was not observed by Bellingeri et al. [22] who have used a different preparation route.

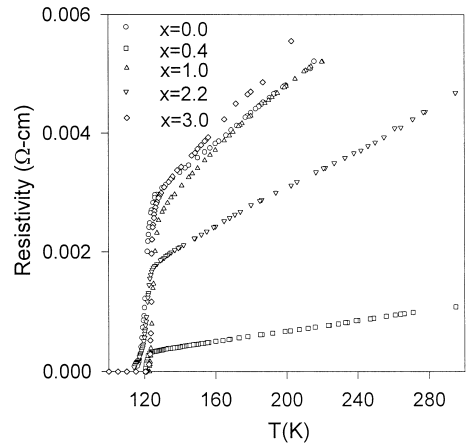


Fig. 5. Variation of the resistivity of different samples with temperature.

The phase diagram of  $T_c$  vs.  $x$  presented in Fig. 6 exhibits anomalous behavior around  $x = 2.2$  that demands further investigations. Attempts are currently going on in our laboratory to control the amount of fluorine that enters the structure.

Fluorine incorporation has been found to enhance the metallic behavior of the n-type Nd-based superconductors [31]. Careful analysis of the variation of the normal state resistivity with temperature (Fig. 5) shows that the fluorine-free sample and samples with

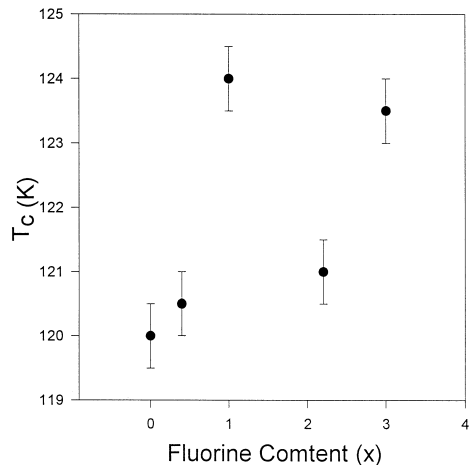


Fig. 6. Variation of the transition temperature  $T_c$  with fluorine content,  $x$ .  $T_c$  was obtained from the peak position in  $(d\rho/dT)$  vs.  $T$ .

low fluorine content are slightly overdoped, with a concave shape. To investigate the doping state in more details, two samples were prepared under the same conditions but annealed in oxygen atmosphere. These samples had fluorine content  $x = 3.0$  and  $x = 3.6$  [33]. Fig. 7 shows the variation of resistivity with temperature for these two samples and for the sample with  $x = 3.0$  annealed in air. The figure clearly shows that the oxygen-annealed sample with  $x = 3.0$  has a concave shape, representing an overdoped state, while the sample with the same fluorine content annealed in air varies almost linearly with temperature and has higher transition temperature. The oxygen-annealed sample with  $x = 3.6$  has almost a linear behavior, indicating that this sample is near optimal doping [3–5,33]. These results are in agreement with the behavior of the resistivity of the overdoped and underdoped TI-based compounds with temperature reported by Ren et al. [33]. The normal state resistivity of the sample with the lowest fluorine content ( $x = 0.4$ ) is considerably lower than that of all other samples. Fluorine inclusion into the structure of TI-1223 reduces the hole concentration which is equivalent to creating an oxygen non-stoichiometric state (annealing in air) and primarily changes the charge carrier concentration in the Cu–O planes of the TI-1223.

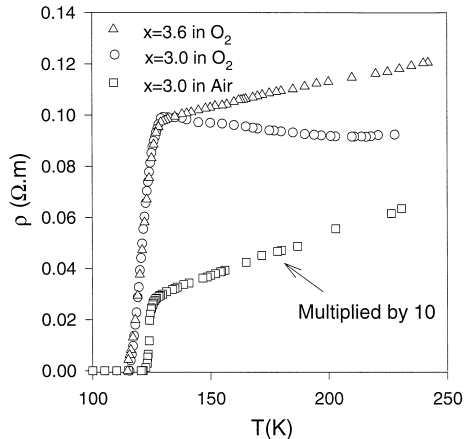


Fig. 7. Typical resistivity dependence on temperature of an overdoped TI-1223 ( $x = 3.0$  annealed in  $O_2$ ) to show the concave shape of the normal state resistivity and that of an almost optimally doped TI-1223 with  $x = 3.6$  annealed in  $O_2$  atmosphere and TI-1223 with  $x = 3.0$  annealed in air both having a linear dependence.

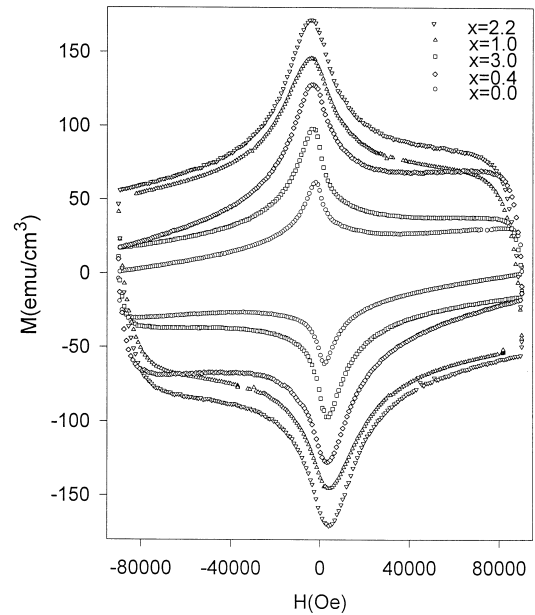


Fig. 8. Zero field-cooled hysteresis loops for samples with different fluorine contents,  $x$ .

### 3.3. Magnetic properties

The zero field-cooled hysteresis loops measured at 4.2 K for samples with various fluorine content are shown in Fig. 8. The figure shows that the width of the hysteresis loops increases with increasing fluorine content, reaching a maximum for  $x = 2.2$ , above which the width starts decreasing. Fig. 9

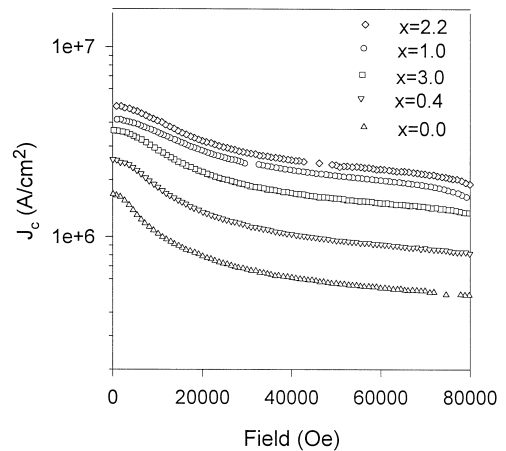


Fig. 9. The critical current density of TI-1223 samples with different fluorine contents, calculated from Bean's model.

shows the variation of critical current density  $J_c$  as a function of field which is calculated from Bean's model, through the relation:

$$J_c \approx -30 \frac{M_+(H) - M_-(H)}{D} = 30 \frac{\Delta M}{D},$$

for  $H_{c1} \ll H \ll H_{c2}$  where  $M_+(H)$ , and  $M_-(H)$  are the magnetization (in emu/cm<sup>3</sup>) measured with increasing and decreasing fields, respectively. The average grain size  $D$  (in cm) [34] is taken to be 20  $\mu\text{m}$  as seen from the SEM micrographs.

The critical current density  $J_c$  for the sample with  $x = 2.2$ , is about 300% of the corresponding value for fluorine-free sample. For  $x = 3$ ,  $J_c$  starts decreasing, reaching about 200%, the value for the sample with  $x = 0$  [23]. This enhancement of the critical current density has not been observed by Bellingeri et al. [22]. The figure also reveals that at low fields, the initial drop in  $J_c$  with increasing field is reduced in fluorinated samples. This is mainly due to the reduction of the weak links between the grains. As a consequence, the inter-grain critical current density becomes less field-dependent. Similar behavior is also observed at higher fields where  $J_c$  has a plateau-like behavior. This further indicates that fluorine addition is affecting grain growth and the pinning mechanism, which results in the reduction of the field dependency of the critical current density. The improvements of the magnetic field dependence of the  $J_c$  are consistent with recent results obtained

for fluorine-doped Tl-1223 [22,23]. In Fig. 10, we present the values of  $J_c$  at 4.2 K and  $H = 1$  T for different fluorine contents. The critical current density gradually increases, reaching a maximum at  $x = 2.2$ , then starts decreasing. This maximum in  $J_c$  does not correspond to the maximum in  $T_c$  (which is at  $x = 1.0$ ). The sample with minimum normal state resistivity and minimum  $c$ -axis showed no anomalous behavior in  $J_c$ , indicating that fluorine addition affected the low-temperature (superconducting) and high-temperature (normal state) properties differently.

#### 4. Conclusions

We have investigated the effect of fluorine on various superconducting and normal state properties of the Tl-1223 superconductors. Direct observation of fluorine in the Tl-1223 phase is achieved for the first time using EDX analysis and was further supported by the reduction of the  $c$ -axis of the Tl-1223 with fluorine addition. Moreover, fluorine addition promotes the formation of the Tl-1223 phase over the Tl-1212 phase, and increases grain size (up to 100  $\mu\text{m}$ ). An increase in the transition temperature associated with a decrease in the transition width has been observed. As fluorine ( $\text{F}^-$ ) replaces oxygen ( $\text{O}^-$ ), the hole concentration in the Cu–O planes will decrease, approaching the optimum value, changing the overall behavior of the normal state resistivity.

The width of the hysteresis loops  $\Delta M$  increases with increasing fluorine content up to 2.2 to 300% of its fluorine-free value, and  $\Delta M$  becomes less field-dependent. This also suggests that fluorine enhances the pinning strength and affects the pinning mechanism.

These improvements in the superconducting and transport properties along with structural changes suggest that fluorine enters the structure of the superconducting Tl-1223 phase, and changes the density of charge carriers in the Cu–O planes.

#### Acknowledgements

The authors would like to acknowledge the support of King Fahd University of Petroleum and

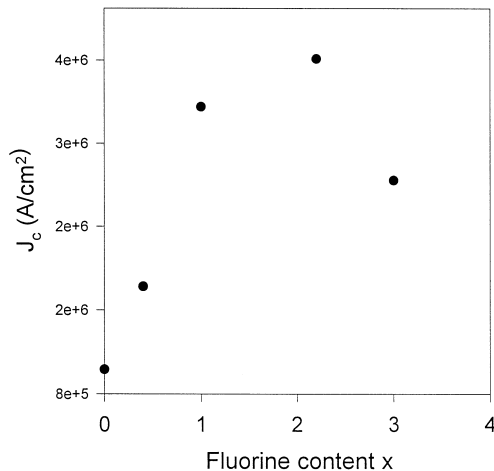


Fig. 10. The critical current density of Tl-1223 samples with different fluorine contents at 1 T.

Minerals. This project was supported in part by SABIC under grant number PH/SABIC 96-2. We are also thankful to Dr. M. Faiz and Dr. J. Shirokoff for useful discussions.

## References

- [1] R.S. Liu, P.P. Edwards, in: A.M. Herman, J.V. Yakhmai (Eds.), *Thallium-Based High Temperature Superconductors*, Marcel Dekker, New York, 1994, pp. 325–346.
- [2] M.A. Subramanian, A.S. Ganguli, in: A.M. Herman, J.V. Yakhmai (Eds.), *Thallium-Based High Temperature Superconductors*, Marcel Dekker, New York, 1994, pp. 347–370.
- [3] M.R. Presland, J.L. Tallon, R.G. Buckley, R.S. Liu, N.E. Flower, *Physica C* 176 (1991) 95.
- [4] M.-H. Pan, M. Greenblatt, *Physica C* 176 (1991) 80.
- [5] M. Paranthaman, A. Manthiram, J.B. Goodenough, in: A.M. Herman, J.V. Yakhmai (Eds.), *Thallium-Based High Temperature Superconductors*, Marcel Dekker, New York, 1994, p. 171.
- [6] S. Nakajima, M. Kikuch, Y. Syono, T. Oku, K. Nagase, N. Kobayashi, D. Shindo, K. Hiraga, *Physica C* 182 (1991) 89.
- [7] S. Nakajima, M. Kikuch, Y. Syono, N. Kobayashi, *Physica C* 185–189 (1991) 673.
- [8] A. Krol, Y.L. Soo, Z.H. Ming, S. Huang, H. Kao, G.C. Smith, K. Lee, A.C.W.P. James, D.W. Murphy, *Phys. Rev. B* 46 (1992) 443–447.
- [9] T. Hamada, R. Morimo, *Phys. Status Solidi A* 151 (1995) 199.
- [10] T. Hamada, T. Nomachi, *Phys. Status Solidi A* 153 (1996) 165.
- [11] F. Sumiyoshi, T. Hamada, S. Kawabata, *Cryogenics* 28 (1988) 3.
- [12] N.P. Bansal, A.L. Sandkuhl, D.E. Farrell, *Appl. Phys. Lett.* 52 (1988) 838.
- [13] P. Massiot, C. Perrin, M. Guilloux-Viry, J.-C. Jegaden, A. Perrin, M. Sergent, *Solid State Commun.* 98 (1996) 501.
- [14] R.V. Shpanchenko, M.G. Rozova, A.M. Abakumov, E.I. Ardashnikova, M.L. Kovba, S.N. Putilin, E.V. Antipov, O.I. Lebedev, G. van Tendeloo, *Physica C* 280 (1997) 272.
- [15] C. Wang, J. Liang, X. Chen, J. Min, G. Rao, C. Dong, G. Che, S. Jia, *Physica C* 260 (1996) 64.
- [16] Y. Hakuraku, F. Sumiyoshi, K. Kittaka, T. Hamada, S. Kawabata, T. Ogushi, *Cryogenics* 29 (1989) 415.
- [17] E. Kemnitz, S. Scheurell, S.W. Naumov, P.E. Kasin, V.I. Pershin, R.K. Kremer, *Eur. J. Solid State Inorg. Chem.* 30 (1993) 701.
- [18] G.B. Peacock, I. Gameson, M. Slaski, J.J. Capponi, P.P. Edwards, *Physica C* 289 (1997) 153.
- [19] K. Tachikawa, Y. Yamada, Kinoshita, *Proceedings of the 1994 Topical International Cryogenic Materials Conference*, Honolulu, HI, USA, World Scientific, Singapore, 1995, p. 311.
- [20] Y. Xin, K.W. Wong, G.F. Sun, D.F. Lu, *Solid State Commun.* 87 (1993) 1065.
- [21] G.F. Sun, Y. Xin, D.F. Lu, K.W. Wong, Y. Zhang, J.G. Stevens, *Solid State Commun.* 101 (1997) 849.
- [22] E. Bellingeri, R. Gladyshevskii, F. Marti, M. Dhalle, R. Flükiger, *Supercond. Sci. Technol.* 11 (1998) 810.
- [23] N.M. Hamdan, Kh.A. Ziq, A.S. Al-Harathi, *J. Low Temperature Phys.* 105 (1996) 1493.
- [24] N.M. Hamdan, A.S. Al-Harathi, M.F. Choudhary, *Physica C* 282–287 (1997) 2273.
- [25] N.M. Hamdan, Kh.A. Ziq, A.S. Al-Harathi, *J. Supercond.* 11 (1) (1998) 95.
- [26] R.E. Gladyshevskii, A. Perin, B. Hensel, R. Flükiger, R. Abraham, K. Lebbou, M.Th. Cohen-Adad, J.L. Jorda, *Physica C* 255 (1995) 113.
- [27] R.E. Gladyshevskii, Ph. Galez, K. Lebbou, J. Allemand, R. Abraham, M. Couach, R. Flükiger, J.-L. Jorda, M.Th. Cohen-Adad, *Physica C* 267 (1996) 93.
- [28] PDP program, ICTP, Trieste, Italy, 1990.
- [29] X. Gao, J. Li, D. Gao, G. Zheng, S. Gao, *Mod. Phys. Lett. Phys. Lett. B* 6 (15) (1992) 943.
- [30] X. Gao, X. Wu, H. Yan, Z. Yin, C. Lin, Y. Fu, W. Xie, *Mod. Phys. Lett. Phys. Lett. B* 4 (15) (1990) 137.
- [31] X.-G. Wang, Z. Huang, L. Yuan, *Physica C* 253 (1995) 245.
- [32] Y.T. Wang, A.M. Hermann, *Physica C* 254 (1995) 1.
- [33] Z.F. Ren, J.H. Wang, D.J. Miller, *Appl. Phys. Lett.* 71 (1997) 1706.
- [34] C.P. Poole Jr., H.A. Farach, R.J. Crewick, *Superconductivity*, Academic Press, San Diego, 1995, p. 389.